J. Chil. Chem. Soc., 58, Nº 4 (2013)

STUDY BASED ON ELECTRONIC DESCRIPTORS OF THE DIASTEREOSELECTIVE AZA-DIELS-ALDER CYCLOADDITION OF [(1R)-10-(N,N-DIETHYLSULFAMOYL)ISOBORNYL] 2H-AZIRINE-3-CARBOXYLATE TO E,E-1,4-DIACETOXY-1,3-BUTADIENE

YASSER B. RUIZ-BLANCO,[a,c] MARIA J.ALVES,[b] JOSÉ E. RODRÍGUEZ-BORGES[c] AND REINALDO MOLINA[d]*

[a]*Unit of Computer-Aided Molecular "Biosilico" Discovery and Bioinformatic Research (CAMD-BIR Unit), Facultad de Qu{imica y Farmacia. Universidad Central "Marta Abreu" de las Villas, Santa Clara, 54830, Villa Clara, Cuba.*

[b]*Departamento de Química, Universidade do Minho, Campus de Gualtar, 4710-057 Braga, Portugal*

[c]*CIQUP, Departamento de Química, Faculdade de Ciências, Universidade do Porto, Rua do Campo Alegre, 687, 4169-007 Porto, Portugal*

[d]*ChemicalBioactives Center, Central University of "Las Villas" 54830, Cuba*

(Received: December 21, 2012 - Accepted: May 28, 2013)

ABSTRACT

Cycloaddition of chiral [(1*R*)-10-(*N*,*N*-diethylsulfamoyl)isobornyl] 2*H*-azirine-3-carboxylate to *E*,*E*-1,4-diacetoxy-1,3-butadiene shows complete diatereoselectivity giving a single cycloadduct (-)-(2*S*,5*R*,6*R*)-6-[(1*R*)-10-(*N*,*N*-diethylsulfamoyl)isobornyloxycarbonyl]-1-azabicyclo[4.1.0]hept-3-ene-2,5-diyldiacetate. Our main objective is to identify electronic/steric parameters capable of describing the observed tendencies of this reaction. The results of the calculations conclude that: even though the steric factors can play an important role at the initial steps of the reaction, at the transition states the behavior of several electronic parameters; like hardness, polarizability, aromaticity, charge transfer, etc is decisive enough to justify the obtained product. Finally, this work summarizes an exhaustive analysis of electronic descriptors and empirical reactivity principles, reaching a definitive and comprehensive explanation to the observed experimental result.

Keywords: Maximum hardness principle; Minimum polarizability principle; reactvity principles; aromaticity of transition states; 2H-azirine-3-carboxylate.

1. INTRODUCTION

Computational studies of complete-diastereoselective cycloadditions are key tasks for indentifying the relative influence of the steric and electronic effects in asymmetric induction. Here, the behavior of several electronic indices for the transition states of the different reaction pathways is analyzed in order to justify the observed diastereoselectivity of the title reaction.

The aza-Diels-Alder cycloadditions are one of the main tools that organic chemists usually use to synthesize six-membered ring of nitrogen containing heterocyclic compounds, many of them with huge potential as synthons to achieve more elaborated molecules including bioactive compounds.[1-3] In this context, electrophilic chiral 2*H*-azirines-3-carboxylates are excellent partners in the Diels-Alder reaction expressing high reactivity, in the absence of catalysts.[4] These reactions yield fused bicyclic nitrogen-containing compounds,[4] with high biological potential, including the synthesis of iminosugars.[5-8]

In a previous work, it was found a complete diastereoselectivity in the reaction of 2*H*-azirine-3-carboxylic acid derivative **1** bearing the [(1*R*)-10-(*N*,*N*-diethylsulfamoyl)isobornyl] auxiliary when reacting with a 1,4-diacetoxy-1,3-diene.[5, 9]The facial selectivity of azirine **1** when reacts with diene **3** yielded a cycloadduct **4** with 2*S*, 5*R*, 6*R* stereocentres configurations, in 54 % yield (Scheme 1). *This result contradicts the general stereo-selectivity trend of the very azirine with other dienes*[9, 10] in which the major isomer is *S* configuration at the chiral carbon of the aziridine ring. In that report it was suggested that some electronic features could be the causes involved in such an unexpected result, *however no evidence was provided about the actual reason of such behavior*.

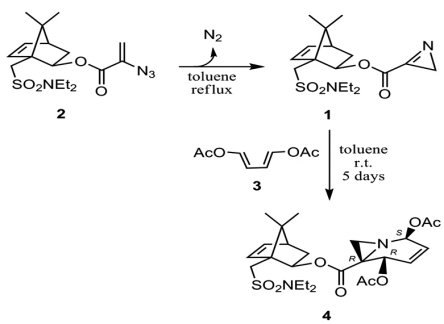

Scheme 1. Scheme of the synthesis yielding the cycloadduct (-)-(2*S*,5*R*,6*R*)-6-[(1*R*)-10-(*N*,*N*-diethylsulfamoyl)isobornyloxycarbonyl]-1-azabicyclo[4.1.0] hept-3-ene-2,5-diyldiacetate (P_*endo-R*).

The structure obtained by X-ray diffraction for the product **4** is shown in Figure 1.[5, 9] The supplementary crystallographic data for this paper can be obtained free of charge from The Cambridge Crystallographic Data Centre, via www.ccdc.cam.ac.uk/data_request/cif, with the deposition number CCDC 723973–723975.

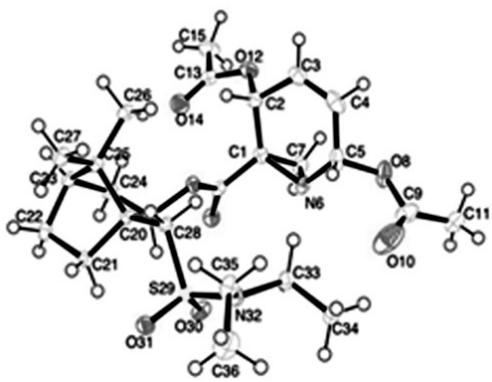

Figure 1. Structure obtained by X-rays diffraction for compound (**4**) (P_*endo-R*).

The purpose of this work is to rationalize the particular stereoselectivity of the mentioned aza-Diels-Alder reaction. There are some electronic indices described in the literature that have proved to have tight relation with the stereoselectivity of Diels-Alder (DA) reactions; that is the case of the popular electrophilicity index defined by Parr *et al.* (1999). Also there are concepts like aromaticity of transition states arrived from the interpretation in Density Functional Theory (DFT) of the Woodward-Hoffmann rules[11, 12] which allows getting an idea of the behaviour of cycloaddition reactions. Hardness is a parameter defined as half of the second derivative of the energy respect to the number of electrons of the system and has a direct relation with the concept of aromaticity;[12-14] this index is also interpreted in terms of the difference in energy of the frontier orbital of the system being in consequence a measure of its stability. This parameter was taken by Pearson in 1987 to enunciate the principle of maximum harness (MHP) as: "there seems to be a rule of nature that molecules arrange themselves so as to be as hard as possible",[15, 16] which was later theoretical analyzed by Parr and Chattaraj (1991).[17] The other principle we

e-mail: yasserrb@uclv.edu.cu

used in this study is known as minimum polarizability principle (MPP) which definition was first stated by Chattaraj*et al.* (1996) as: "the natural direction of evolution of any system is towards a state of minimum polarizability".[18] *These principles constitute valuable tools for the analysis of reactivity and selectivity of chemical reactions and particularly of aza-DA cycloaditions*.

The study of reaction mechanisms implies, frequently, a time-consuming and resource-demanding simulation. Using the above electronic parameters avoid complex steps like the optimization of molecular complexes which are usually difficult to obtain given the common planarity of the potential energy hyper-surface.

2. Methods: Electronic descriptors

Global electronic indices, as the defined within the DFT of Parr, Pearson, and Yang[19, 20] are useful tools to understand the reactivity of molecules in their ground states. In this section we briefly present several electronic descriptors that were used in this work. For instance, the electronic chemical potential, μ, describing the changes in electronic energy with respect to the number of electrons is usually associated with the charge-transfer ability of the system in its ground-state geometry. It has been given a very simple operational formula in terms of the one electron energies of the frontier molecular orbital HOMO and LUMO, ε_H and ε_L, as:

$$\mu \approx \frac{\varepsilon_H + \varepsilon_L}{2} \qquad (1)$$

A quantitative representation of the chemical hardness concept, η, introduced by Pearson,[21] see introduction section, it is the approximate expression:[22]

$$\eta \approx \frac{\varepsilon_H - \varepsilon_L}{2} \qquad (2)$$

Parr *et al.*[23] have introduced a new and useful definition of global electrophilicity, which measures the stabilization in energy when the system acquires an additional electronic charge from the environment. The electrophilicity power, ω, has been given the following simple expression:

$$\omega = \frac{\mu^2}{2\eta} \qquad (3)$$

in terms of the electronic chemical potential, μ, and the chemical hardness, η, defined in equations **1** and **2**. The difference of this index between reactants is taken as a measure of the polarity of the cycloaddition.[24]

While the electrophilicity index measure the effect of an electron transfer from an undefined environment, the initial electron transfer index, ΔN, provides an approach to the electron transfer between two reactants in the initial steps of the reaction path, this parameter is expressed in the next way:

$$\Delta N \approx \frac{\phi_A - \phi_B}{2(\eta_A + \eta_B)} \qquad (4)$$

Where $\phi_A, \phi_B, \eta_A, \eta_B$ are the dipolar moments and hardness of both reactants. Small values of this index are associated with *low orbital interactions* between reactants and thus a domain of the *electrostatics ones*

Another global parameter that we studied in this work is the mean polarizability, α. When a molecule is embedded in a uniform electric field, E_o, in vacuum, an induced dipole moment, ϕ_{IND}, comes up defined by the relationship:

$$\phi_{IND} = \alpha E_0 \qquad (5)$$

in which the scalar constant of proportionality, α, is called polarizability (or static polarizability). In general, the scalar polarizability not sufficient to describe the induced polarization, therefore, a polarizability tensor is used to better encode the induced polarization and represents molecular polarizability. The mean polarizability, $\hat{\alpha}$, of a molecule is calculated by the relation expressed below:[22]

$$\hat{\alpha} = \frac{\alpha_{xx} + \alpha_{yy} + \alpha_{zz}}{3} \qquad (6)$$

in which the numerator is the summation of the polarizabilities along each principal component axis of the molecule, obtained by diagonalization of the polarizability tensor. Each component of the polarizability tensor α'_{xx}, α'_{xy}, α'_{yy}, α'_{xz}, α'_{yz} and α'_{zz} are given by Gaussian in a frequency calculation output with the keywords "Exact Polarizability".

The extent of bond formation along a reaction pathway is provided by the concept of bond order. This theoretical tool has been used to study the molecular mechanism of chemical reactions.[25] To follow the nature of these processes, the Wiberg bond indexes[26] have been computed by using the NBO[27-29] population analysis as implemented in Gaussian03. **Methods: Computational Details**

All calculations were carried out with the Gaussian03 suite of programs[30] at both rHF/6-31G (d, p) and rB3LYP/6-31G (d, p) levels. The Berny analytical gradient optimization method[31, 32] was used for all geometries optimizations. Products and reactants were optimized first; the best conformer was found for the azirine derivative and the diene was optimized at *s-cis* conformation. The stationary points were characterized by frequency calculations in order to verify that minima and transition structures have zero and one imaginary frequency, respectively. The intrinsic reaction coordinate (IRC)[33] paths were traced in order to check the energy profiles connecting each transition structure to the two associated minima of the proposed mechanism, by using the second-order González-Schlegel integration method.[34, 35] The electronic structure of the transitions states were analyzed using the natural bond orbital (NBO) method.[36, 37] Solvent effects have been considered by single points calculations using a relatively simple self-consistent reaction field (SCRF)[38, 39] based on the polarizable continuum model (PCM) developed by Tomasi's group.[40, 41] The solvent employed was toluene as it was used in the synthesis. Zero point corrections were calculated for each stationary point of the reaction path. The chemical potential, hardness and electrophilicity indices were estimated using frontier molecular orbitals.[24, 42-45]

3. RESULTS AND DISCUSSION

The reactant's system is characterized by a low initial charge transfer index, ΔN, as well as a low difference in the electrophilicity index, $\Delta\omega$, from the diene towards the dienophile, see Table 1.

Table 1. Global electronic indices for reactants.

	η (a.u.)	μ (a.u.)	ω (eV)	ΔN (a.u.)	$\Delta\omega$ (eV)
Diene	0,0908	-0,126	2,39	0,093	1,66
Dienophile	0,0851	-0,159	4,05		

These features are typical for medium polar cycloadditions with normal electron demand orientation, where the electrostatic/steric interactions in the initial part of the mechanism have an overweight in comparison with the orbitalic ones. *This analysis shed some light about the important role of the large bicyclic group of the dienophile in the course of the reaction.*

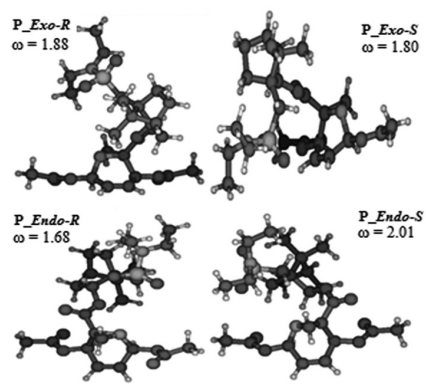

Figure 2. Geometries of the four possible products of the cycloaddition obtained with DFT calculations. The absolute configuration taken to identify the structures is associated with the chiral carbon of the aziridine ring. The value of the electrophilicity index, in eV, for each product is exposed aside.

The reaction has four possible products, see Figure 2, which result through the TSs shown in Figure 4. The values of the electrophilicity index, shown in Figure 2, are in agreement with the result obtained by Noorizadeh and Maihami; they have investigated the selectivity of 67 cycloadditions using the electrophilicity index of the reaction products, and found that the major product always had a *lesser electrophilicity value*.[46]

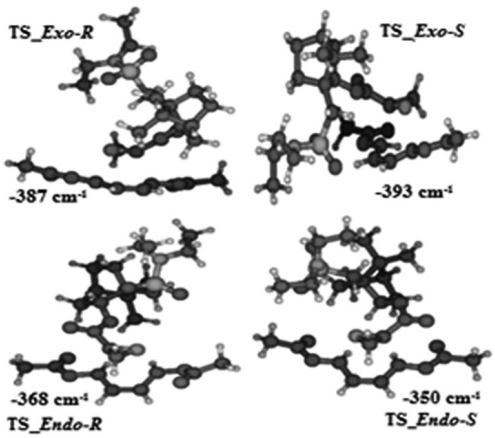

Figure 3. Representation of the transition state's geometries, and their negative wave numbers. Geometries and wave numbers were taken from DFT calculations.

All TSs were calculated and characterized at HF and DFT, the geometries of the structures obtained with DFT are given in Figure 3 joined with their negative wave number. All the IRCs share the same form, see Figure 4 as an example, first a slight increase towards the TSs and then a nicely decrease until the products. This result in conjunction with the interatomic distances, Table 2, suggests a concerted slightly asynchronous mechanism.

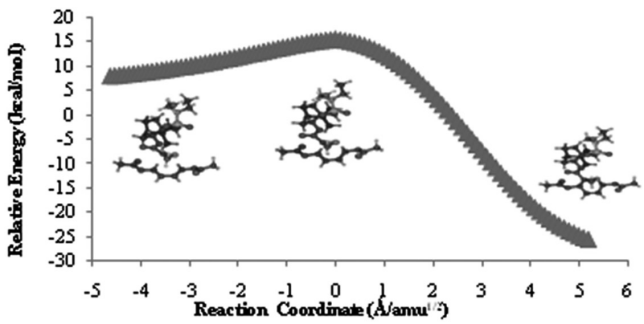

Figure 4. rB3LYP/6-31G (d, p) IRC plot of the *endo-R* approach channel of the cycloaddition.

2.1 Aromaticity analysis in transition states

The distance's values reported in Table 2 reflect a high similarity between the distances of both forming bonds in all TSs, but the TS_*endo-R*. Such feature should imply stronger interactions between the carbons, of the C—C forming bond, in all the TSs, except in the TS_*endo-R* where the shorter C—N length suggests more balanced interactions between both forming bonds. This statement is supported by the larger population of the LUMO of the dienophile over the carbon than over the nitrogen in the C=N bond; as shows Figure 5, thus with similar interaction's distances the C—C interaction must be stronger due to its larger overlapping between the frontier orbitals.

According with the above simple analysis, the TS_*endo-R* belongs to the most synchronic reaction path, which is in agreement with a larger aromaticity and thus stability. The electronic charge transferred, in solution, for all the TSs were calculated using natural bond orbital (NBO) analysis at both levels of theory, see Table 2. This quantity offers another evidence of the medium polar character of the cycloaddition, because its moderated values agree with the larger synchronicity of TS_*endo-R* and therefore its *larger aromaticity*.

Figure 5. Representation of the LUMO of the dienophile and the HOMO of the diene.

Table 2. Wiberg's bond indices and spatial distances of the forming bonds in the cycloaddition and electronic charge transfer values from the diene to the dienophile.

Systems	HF		DFT	
Distances (Å)	**C—C**	**C—N**	**C—C**	**C—N**
TS_*exo-S*	2.13	2.16	2.24	2.16
TS_*endo-S*	2.17	2.15	2.28	2.20
TS_*exo-R*	2.12	2.18	2.22	2.20
TS_*endo-R*	**2.22**	**2.06**	**2.34**	**2.11**
Bond indices				
TS_*exo-S*	0.364	0.294	0.302	0.318
TS_*endo-S*	0.362	0.300	0.299	0.294
TS_*exo-R*	0.367	0.280	0.305	0.293
TS_*endo-R*	**0.328**	**0.345**	**0.267**	**0.336**
Chargetransfers (a. u.)				
TS_*exo-S*	0,228		0.211	
TS_*endo-S*	0.226		0.211	
TS_*exo-R*	0.226		0.212	
TS_*endo-R*	**0.161**		**0.160**	

Analysis of second order interactions with NBO, Table 3, also demonstrate the synchronicity and *aromaticity* of TS_*endo-R*, evidenced in the lower difference of the stabilization energy of the interactions between the natural bonding (BD) and antibonding (BD*) orbitals in both cycloaddition's extremes, $|\Delta E_{BD\text{-}BD^*}|$. The similarity of such interactions in the extremes of the cycloaddition centre is a key proof for the aromatic character of the TSs and particularly of TS_*endo-R*. Such result agrees with the thought that conversely to highly polar cycloadditions, where Michael type attacks are probable, in medium polar ones the process is enhanced by *highly synchronic and aromatic TSs*.

Table 3. Difference of stabilization energy (|ΔE|) of the interactions between bonding orbitals(BD), lonepairs (LP), and antibonding orbitals (BD*) in the reactions centres.

Method	*Systems*	$\lvert\Delta E_{BD\text{-}BD^*}\rvert$	$E_{LP\text{-}BD^*}$
HF	**TS_*exo-S***	51.70	13.06
	TS_*endo-S*	42.70	15.97
	TS_*exo-R*	54.37	11.85
	TS_*endo-R*	**17.04**	**22.36**
DFT	**TS_*exo-S***	13.19	8.88
	TS_*endo-S*	11.45	8.99
	TS_*exo-R*	15.22	7.48
	TS_*endo-R*	**1.25**	**13.07**

Another interesting magnitude obtained from the NBO analysis is the stabilization energy related to the interaction of the lone pair (LP) of the nitrogen of the azirine with an antibonding natural bond orbital in the nearest extreme of the diene $\mathbf{E}_{LP\text{-}BD^*}$. This quantity exhibits its larger value in the TS_*endo-R*. The effect of such interaction over the stereoselectivity of the cycloaddition could be understood under the aromaticity theory considering that *this interaction acts as a stabilising factor of the aromatic system*. The interaction of this electron pair with the π system decreases the net charge transfer from diene to dienophile lowering the difference of the chemical potential between the two entities, and therefore biasing the reactions through the TS_*endo-R*. The values of the Wiberg bond indices, see Table 2, entirely support the effect of such interaction between azirine's nitrogen and the nearest carbon atom of the diene, showing a larger electron sharing between these two atoms than between both carbon atoms of the other forming bond.

1.2 Polarizability analysis in transition states

From the MPP, see introduction section, a reaction path would be favored if it takes place through the TS with minimum polarizability. The numbers in Table 4 show that TS_*endo-R* has a *low value of mean polarizability*, only the TS_*exo-S* presents a lower one with DFT. The analysis of this property on the basis of the minimum polarizability principle provides another suitable judgment element to understand the favored character of TS_*endo-R*.

Table 4. Mean polarizability values, â, and chemical hardness values, η, (in a. u.) for every TS.

	HF		***DFT***	
	â	***η***	***â***	***η***
TS_*endo-R*	**320.442**	**0.2016**	361.849	**0.0846**
TS_*endo-S*	323.406	0.1964	364.068	0.0830
TS_*exo-R*	321.034	0.1961	361.868	0.0830
TS_*exo-S*	320.720	0.1969	361.208	0.0836

In this case the continuous model of DFT together with the use of diffuse functions in the basis set leads to a possible overestimation of the polarizabilities and is not surprising some changes are obtained in the order of the system with quite similar polarizability values. Note that, in spite of this, a general tendency actually can be inferred from the polarizability values of both techniques: i.e. TS_endo-R and TS_exo-S are those with lowest polarizability whereas the other two show definitely higher values of this parameter.

The joint use of both methods, HF and DFT, in the present paper is not just in order to compare their respective results but also to perform a coupled analysis of these results. None of these methods can be considered better than the other for all purposes and systems, and particularly in the present study, dealing with stereoselectivity, fine differences and even contradictory values could be expected for a particular test thus our strategy was to achieve a multi-objective analysis proposing a final consensual result.

2.3 Hardness analysis in transition states

Chemical hardness is inversely related to polarizability. According to the maximum hardness principle the reaction path with the hardest TS should be biased along the reaction. Table 4 summarizes the values of hardness for the different TSs. The *larger value of* TS_*endo*-R *indicates the highest reactivity of this transition state*.

The results of the three electronic features described until this point provide individually but mostly in conjunction a defined vision of the relative reactivity of each TS and thus constitute a clear justification of the stereoselectivity of the cycloaddition.

1.4 Energetic and solvent effect analysis

Table 5 and 6 summarizes the absolute and relative energies for reactants, TSs and products of the different reaction paths in vacuum and toluene respectively. Here it is necessary to consider that activation and reaction energies cannot be accurately estimated without obtaining the molecular complexes (MCs), due to such energies are relative parameters of the TSs and products, respectively, related to the MCs not to reactants. However the inverse activation energy can be precisely calculated, agreeing with the experimental results. *The inverse activation energies values (relative values between TSs and products) show a deeper local minima for* P_*endo-R*; this parameter indicates a large kinetic trap and thus irreversibility for P_*endo-R*.

Results obtained in the gas phase are corroborated with the inclusion of the solvent in single point calculations. The solvent (toluene, $\epsilon = 2.38$) stabilizes the reactants system more than the TSs due to its lower polar character in comparison with the reactants. This polarity tendency is exemplified with the dipole moment of TS_*endo-R* (4,83 D), and the summation of the corresponding quantities for both reactants (7,56 D), these values were obtained with DFT. The solvent effect also stabilizes more the reactants than the products (5.13 D for P_*endo-R*) therefore a decrease in the exothermicity of the reaction is obtained in solution. Thus the solvent introduces no significant selectivity between the different cycloaddition paths.

Table 5. Absolute and relative energies[a] for each stationary point of the different reaction paths in vacuum.

	HF			**DFT**		
	E (a. u.)	**$\Delta E_{X\text{-}R}$** (kcal/mol)	**$\Delta E_{TS\text{-}P}$** (kcal/mol)	**E** (a. u.)	**$\Delta E_{X\text{-}R}$** (kcal/mol)	**$\Delta E_{TS\text{-}P}$** (kcal/mol)
Diene	-608.230			-611.766		
Dienophile	-1465.818			-1473.162		
Diene+Dienophile	-2074.048	0,000		-2084.928	0.000	
TS_*endo-R*	-2073.983	42.231		-2084.903	17.029	
P_*endo-R*	-2074.115	**-36.637**	**78.868**	-2084.986	-31.695	**48.724**
TS_*endo-S*	-2073.973	48.398		-2084.899	19.889	
P_*endo-S*	-2074.100	-27.905	76.303	-2084.975	-24.819	44.709
TS_*exo-R*	-2073.985	40.887		-2084.906	15.457	
P_*exo-R*	-2074.111	-34.291	75.178	-2084.987	-32.420	47.876
TS_*exo-S*	-2073.989	38.454		-2084.909	13.089	
P_exo-*S*	-2074.113	-35.758	74.212	-2084.987	-32.450	45.539

$\Delta E_{X\text{-}R}$ is relative to isolated reactants; $\Delta E_{TS\text{-}P}$ is between TSs and products (inverse activation energies). Energies include the zero-point vibrational correction.

Table 6. Absolute and relative energies[a] for each stationary point of the different reaction paths in toluene.

HF				DFT		
	E (a. u.)	ΔE_{X-R} (kcal/ mol)	ΔE_{TS-P} (kcal/mol)	**E** (a. u.)	ΔE_{X-R} (kcal/mol)	ΔE_{TS-P} (kcal/ mol)
Diene	-608.237			-611.772		
Dienophile	-1465.826			-1473.168		
Diene+ Dienophile	-2074.063	0,000		-2084.940	0.000	
TS_*endo-R*	-2073.993	45.261		-2084.912	18.976	
P_*endo-R*	-2074.127	**-34.911**	**80.172**	-2084.995	-29.949	**48.925**
TS_*endo-S*	-2073.983	51.639		-2084.907	22.404	
P_*endo-S*	-2074.112	-25.626	77.266	-2084.984	-23.019	45.423
TS_*exo-R*	-2073.996	43.373		-2084.915	17.336	
P_*exo-R*	-2074,123	-32.006	75.379	-2084.996	-30.633	47.969
TS_*exo-S*	-2073.999	41.513		-2084.917	15.581	
P_exo-*S*	-2074.125	-33.943	75.456	-2084.996	-30.874	46.455

ΔE_{X-R} is relative to isolated reactants; ΔE_{TS-P} is between TSs and products (inverse activation energies). Energies include the zero-point vibrational correction.

4. CONCLUSIONS

Finally the theoretical calculations at rhf/6-31G (d, p) and rb3lyp/6-31G (d, p) levels allowed us to characterize the reactions pathways leading to the four possible diastereoisomeric products of the cycloaddition studied. Global analysis of aromaticity, polarizability and chemical hardness enable justifying the complete stereoselectivity of the studied cycloaddition which is in tight agreement with both, the minimum polarizability and maximum hardness principles. The steric factors seem to play an important role at the initial steps of the reaction; but at the transition states the behavior of several electronic parameters is decisive enough to justify the obtained product. The analysis of the intrinsic reaction coordinate as well as the aromaticity of TSs suggests that the reactions proceed by a concerted slightly asynchronous mechanism. An alternative study was carried out proving that is possible to study reaction mechanisms with a multi-objective analysis of electronic descriptors which is a less time-consuming and computer-resource-demanding strategy, avoiding troublesome steps like determining molecular complexes. Finally, this work summarizes an exhaustive analysis of electronic descriptors and empirical reactivity principles, reaching a definitive and comprehensive explanation to the observed experimental result.

ACKNOWLEDGMENTS

Thanks to Fundação para a Ciência e Tecnologia (FCT) for partial financial support (project PTDC/QUI/67407/2006)

REFERENCES

1. J. E. Rodríguez-Borges, M. L. C. Vale, F. R. Aguiar, M. J. Alves,X. G. Mera, *Synthesis* **6**, 971,(2008).
2. Y. Arroyo, J. F. Rodriguez, M. Santos, M. A. S.Tejedor, I. Vaca,J. L. G. Ruano, *Tetrahedron: Asymmetry* **15**, 1059,(2004).
3. H. H. Jensen, L. Lyngbye, A. Jensrn,M. Bols, *Chem. Eur. J.* **8**, 1218,(2002).
4. M. J. Alves,T. L. Gilchrist, *J. Chem. Soc. Perkin Trans* **1**, 299,(1998).
5. M. J. Alves, C. Costa,M. M. Durães, *Tetrahedron: Asymmetry* **20**, 1378,(2009).
6. R. A. Dwek, T. D. Butters, F. M. Platt,N. Zitzmann, *Nat. Rev. Drug Disc.* **1**, 65,(2002).
7. P. Greimel, J. Spreitz, A. E. Stutz,T. M. Wrodniggm, *Curr. Top. Med. Chem.* **3**, 513,(2003).
8. M. J. Alves, F. T. Costa, V. C. M. Duarte, A. G. Fortes, J. A. Martins,N. M. Micaelo, *J. Org. Chem.* **76**, 9584,(2011).
9. M. J. Alves, J. F. Bickley,T. L. Gilchrist, *J. Chem. Soc. Perkin Trans* **1**, 1399,(1999).
10. Y. S. P. Álvares, M. J. Alves, N. G. Azoia, J. F. Bickley,T. L. Gilchrist, *J. Chem. Soc. Perkin Trans* **1**, 1911,(2002).
11. F. D. Proft, P. W. Ayers, S. Fias,P. Geerlings, *J. Chem. Phys.* **125**, 214101,(2006).
12. Z. Zhou,R. G. Parr, *J. Am. Chem. Soc.* **112**, 5720,(1990).
13. Z. Zhou, R. G. Parr,J. F. Garst, *Tetrahedron Lett.* **29**, 4843,(1988).
14. Z. Zhou,R. G. Parr, *J. Am. Chem. Soc.* **111**, 7371,(1989).
15. R. G. Pearson, *J. Chem. Educ.* **64**, 561,(1987).
16. R. G. Pearson, *Acc. Chem. Res.* **26**, 250,(1993).
17. R. G. Parr,P. K. Chattaraj, *J. Am. Chem. Soc.* **113**, 1854,(1991).
18. P. K. Chattaraj,S. Sengupta, *J. Phys. Chem.* **100**, 16126,(1996).
19. R. G. Parr,W. Yang. Density Functional Theory of Atoms and Molecules; Oxford University Press: New York, 1989.
20. R. G. Parr,R. G. Pearson, *J. Am. Chem. Soc.* **105**, 7512,(1983).
21. R. G. Pearson. Chemical Hardness: Applications from Molecules to Solids; Wiley-VHC: Germany, 1997.
22. R. Todeschini,V. Consonni. Handbook of Molecular Descriptors; WILEY-VCH, 2000.
23. R. G. Parr, L. Szentpaly,S. Liu, *J. Am. Chem. Soc.* **121**, 1922,(1999).
24. L. R. Domingo, M. J. Aurell, P. Perez,R. Contreras, *Tetrahedron* **58**, 4417,(2002).
25. L. R. Domingo, M. Arno, R. Contreras,P. Pérez, *J Phys Chem A* **106**, 952,(2002).
26. K. B. Wiberg, *Tetrahedron* **24**, 1083,(1968).
27. F. Weinhold, *Encycl. Comput. Chem.* **3**, 1793,(1998).
28. A. E. Reed,F. Weinhold, *J. Chem. Phys.* **78**, 4066,(1983).
29. J. P. Foster,F. Weinhold, *J Am Chem Soc* **102**, 7211,(1980).
30. M. J. Frisch. GAUSSIAN 03; Gaussian Inc.: C. T. Wallingford, 2004.
31. R. Hoffmann,R. B. Woodward, *Acc. Chem. Res.* **1**, 17,(1968).
32. R. B. Woodward,R. Hoffmann, *Angewandte Chemie International Edition* **8**, 781,(1969).
33. K. Fukui, *J. Phys. Chem.* **74**, 4161,(1970).
34. C. González,H. B. Schlegel, *J. Phys. Chem.* **94**, 5523,(1990).
35. C. González,H. B. Schlegel, *J. Chem. Phys.* **95**, 5853,(1991).
36. A. E. Reed, R. B. Weinstock,F. Weinhold, *J. Chem. Phys.* **83**, 735,(1985).
37. A. E. Reed, L. A. Curtiss,F. Weinhold, *Chem. Rev.* **88**, 899,(1988).
38. J. Tomasi,M. Persico, *Chem. Rev.* **94**, 2027,(1994).
39. B. Y. Simkin,I. Sheikhet. Quantum Chemical and Statistical Theory of Solutions-A Computational Approach; Ellis Horwood: London, 1995.
40. M. Cossi, V. Barone, R. Cammi,Tomasi, *J. Chem. Phys. Lett.* **255**, 327,(1996).
41. M. T. Cances, V. Mennunci,J. Tomasi, *J. Chem. Phys.* **107**, 3032,(1997).
42. F. Teixeira, J. E. Rodríguez-Borges, A. Melo, M. Natália,D. S. Cordeiro, *Chem. Phys. Lett.* **477**, 60,(2009).
43. L. R. Domingo, *Tetrahedron* **58**,(2002).
44. L. R. Domingo, M. Arnó, R. Contreras,P. Pérez, *J. Phys. Chem. A* **106**, 952,(2002).
45. L. R. Domingo, J. A. Saéz,P. Pérez, *Chem. Phys. Lett.* **438**, 341,(2007).
46. S. Noorizadeh,H. Maihami, *J. Mol. Struct.* **763**, 133,(2006).